Supporting Information

Universal Platform for Ratiometric Sensing based on Catalytically Induced Inner-Filter Effect by Cu^{2+}

Yongchao Fan,[a,b] Huanhuan Xing,[a,b] Yuan Xue,[a,b] Chao Peng,[a,b] Jing Li,[a,b,*] Erkang Wang[a,b,*]

[a] State Key Laboratory of Electroanalytical Chemistry, Changchun Institute of Applied Chemistry, Chinese Academy of Sciences, Changchun, Jilin, 130022, P. R. China

[b] University of Science and Technology of China, Hefei, Anhui, 230026, P. R. China

Corresponding author: Prof. Jing Li and Prof. Erkang Wang*, Tel: +86-431-85262003, Email: lijingce@ciac.ac.cn and ekwang@ciac.ac.cn

Table of contents:

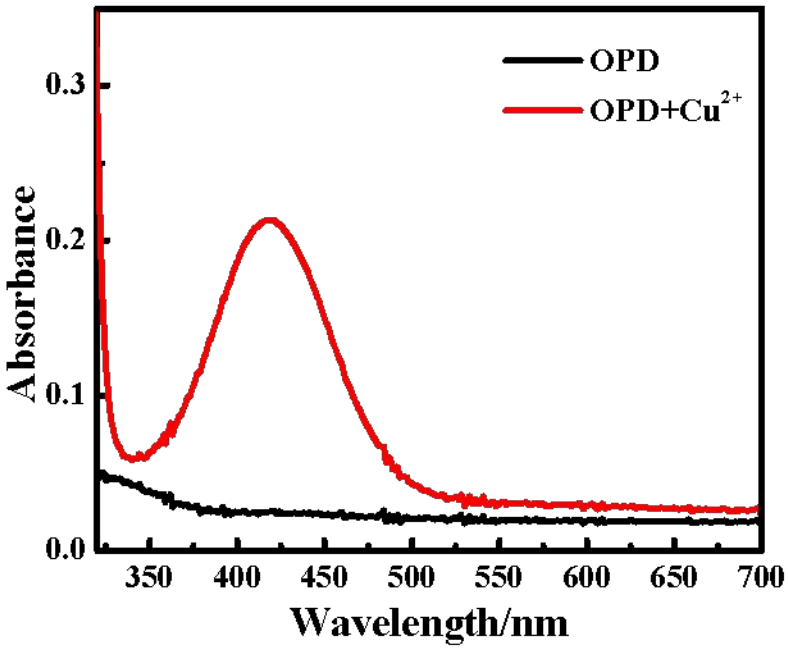

Figure S1. The UV–vis absorption peak at 417 nm of OPD+Cu^{2+}

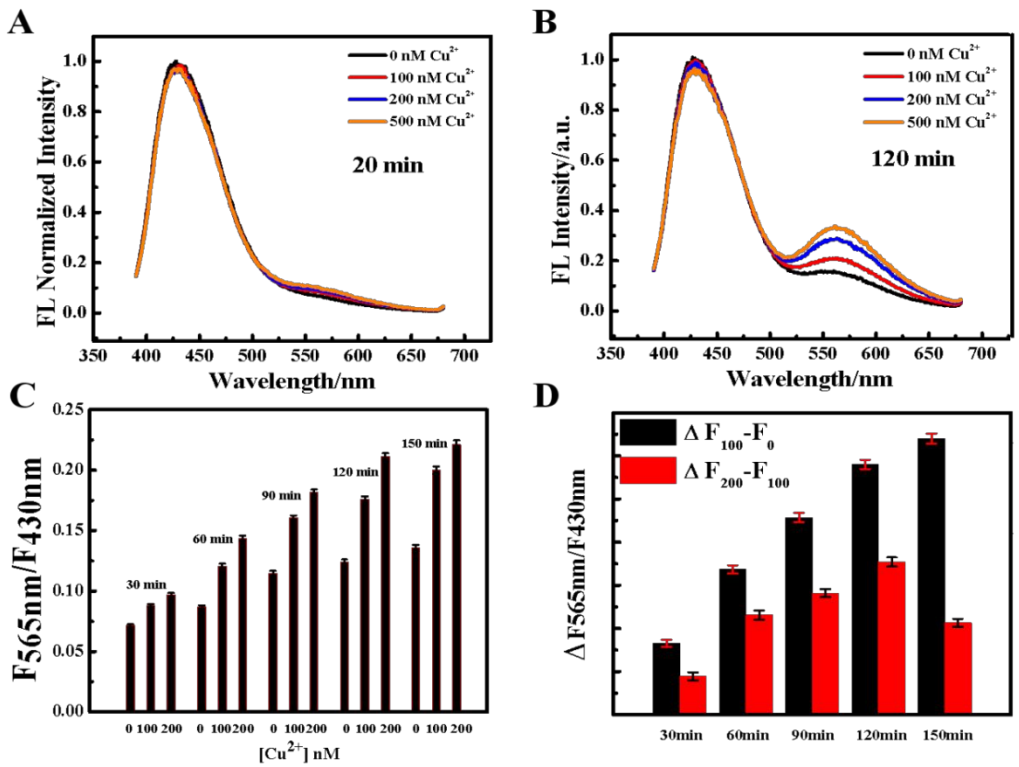

Figure S2. (A) The fluorescence curve of Cu^{2+} concentration of 0 nM, 100 nM, 200 nM, 500 nM with reaction time of 20 min. (B) The fluorescence curve of Cu^{2+} concentration of 0 nM, 100 nM, 200 nM, 500 nM with reaction time of 120 min. (C) The F_{565}/F_{430} of Cu^{2+} concentration 0 nM, 100 nM, 200 nM change with the reaction time from 30 min, 60 min, 90 min, 120 min, 150 min. (D) The difference in F_{565}/F_{430} between the Cu^{2+} concentration of 100 nM and 0 nM (black), the difference in F_{565}/F_{430} between the Cu^{2+} concentration of 200 nM and 100 nM (red).

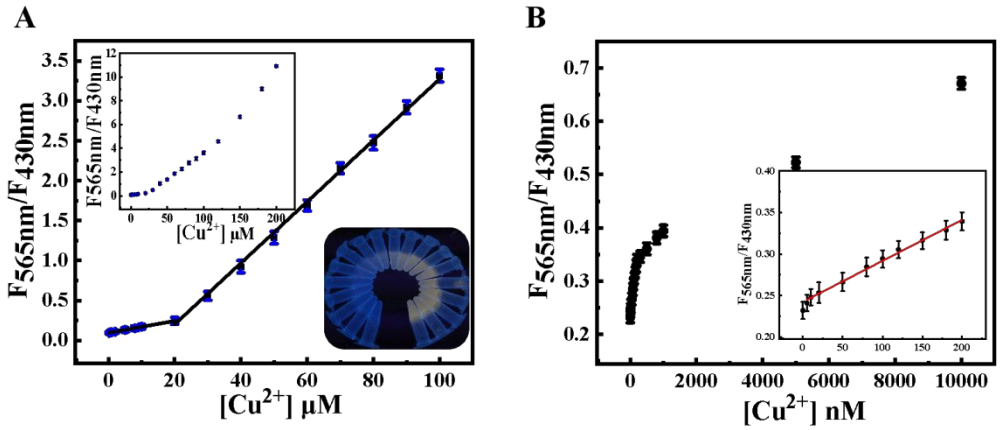

Figure S3. (A) The linear relationship of F_{565}/F_{430} against different concentrations of Cu^{2+} from 0 - 20 μM ($F_{565/430}$ = 0.0074 [Cu^{2+}] (μM) + 0.095, R^2=0.997) and 20 - 100 μM ($F_{565/430}$ =0.0384 [Cu^{2+}] (μM) - 0.567, R^2=0.998). (Illustrations are a change relationship of F_{565}/F_{430} against Cu^{2+} concentration from 0 μM to 200 μM and fluorescence photo of corresponding concentration samples under 365 nm UV light). (B) The linear relationship of F_{565}/F_{430} against different concentrations of Cu^{2+}. (Illustration is a change relationship of F_{565}/F_{430} against Cu^{2+} concentration from 0 nM to 200 nM).

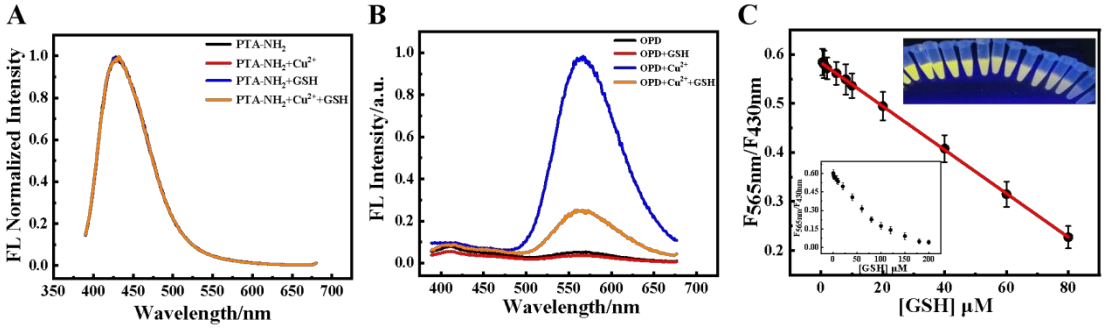

Figure S4. (A) (B) The influence of GSH on the fluorescent response of individual PTA-NH_2 and DAP. (C) The linear relationship of the sensing system against GSH:

The concentrations of GSH are 0.5, 1, 2, 5, 10, 20, 40, 60, 80 μM (Illustration is a change relationship of F_{565}/F_{430} against GSH concentration from 0.1 μM to 200 μM).

Table S1. Compare our work with other reported methods for the detection of Cu^{2+}

Method	Sensing system	LOD (nM)	Detection range (nM)	Ref.
Fluorometry	NH_2-MIL-101 (Al)@ZIF-8	170	1.5×10^3-6.25×10^5	1
Colorimetry	Functional filter paper	33.6	33.6-3.98×10^4	2
Fluorometry	Mesoporous silica	85	not given	3
Fluorometry	CdTe/Silica/Au NCs	410	600-1×10^4	4
Fluorometry	Ce(III)/Tb(III)-Doped SrF_2 NCs	2.2	1-10	5
Fluorometry	Gold nanorods	10	10-300	6
Fluorometry	Ratiometric Sensing PTA-NH_2/OPD	1.7	5-200, 500-2×10^4	this work

Table S2. Compare our work with other reported methods for the detection of

Method	Sensing system	LOD (μM)	Detection range (μM)	Ref.
Fluorometry	MnO_2 nonosheet/ Ir(III) complex	0.13	1-200	7
Colorimetry	AuNPs and CQDs	0.05	1.0 -4.0	8
Fluorometry	g-C_3N_4 NS – MnO_2 Sandwich Nanocomposite	0.2	not given	9
Fluorometry	silver nanoclusters	0.38	0.5-6.0	10
Fluorometry	Fe_3O_4@PFR	0.5	0.8-10	11
Fluorometry	Ratiometric Sensing PTA-NH_2/OPD	0.16	0.5-80	this work

REFERENCES

(1) Zhang, L.; Wang, J.; Ren, X.; Zhang, W.; Zhang, T.; Liu, X.; Du, T.; Li, T.; Wang, J. Internally extended growth of core–shell NH_2-MIL-101(Al)@ZIF-8 nanoflowers for the simultaneous detection and removal of Cu(II)†. *J. Mater. Chem. A* **2018**, *6*, 21029-21038.

(2) Li, J. J.; Ji, C.H.; Hou, C. J.; Huo, D. Q.; Zhang, S. Y.; Luo, X. G.; Yang, M.; Fa, H.B.; Deng, B. High efficient adsorption and colorimetric detection of trace copper ions with a functional filter paper. *Sensor. Actuat. B: Chem.* **2016**, *223*, 853-860.

(3) Chatterjee, S.; Gohil, H.; Raval, I.; Chatterjee, S.; Paital, A. R. An Anthracene Excimer Fluorescence Probe on Mesoporous Silica for Dual Functions of Detection and Adsorption of Mercury (II) and Copper (II) with Biological In Vivo Applications. *Small* **2019**, *15*, e1804749

(4) Wang, Y. Q.; Zhao, T.; He, X. W.; Li, W. Y.; Zhang, Y. K. A novel core-satellite CdTe/Silica/Au NCs hybrid sphere as dual-emission ratiometric fluorescent probe for Cu^{2+}. *Biosens. Bioelectron.* **2014**, *51*, 40-4.

(5) Sarkar, S.; Chatti, M.; Adusumalli, V. N.; Mahalingam, V. Highly Selective and Sensitive Detection of Cu^{2+} Ions Using Ce(III)/Tb(III)-Doped SrF_2 Nanocrystals as Fluorescent Probe. *ACS Appl. Mater. Interfaces* **2015**, *7*, 25702-25708.

(6) Wang, S.; Chen, Z.; Chen, L.; Liu, R.; Chen, L. Label-free colorimetric sensing of copper(II) ions based on accelerating decomposition of H_2O_2 using gold nanorods as an indicator†. *Analyst* **2013**, *138*, 2080-2084.

(7) Dong, Z. Z.; Lu, L.; Ko, C. N.; Yang, C.; Li, S.; Lee, M. Y.; Leung, C. H.; Ma, D. L. A MnO_2 nanosheet-assisted GSH detection platform using an iridium(III) complex as a switch-on luminescent probe†. *Nanoscale* **2017**, *9*, 4677-4682.

(8) Shi, Y.; Pan, Y.; Zhang, H.; Zhang, Z.; Li, M. J.; Yi, C.; Yang, M. A dual-mode nanosensor based on carbon quantum dots and gold nanoparticles for discriminative detection of glutathione in human plasma. *Biosens. Bioelectron.* **2014**, *56*, 39-45.

(9) Zhang, X. L.; Zheng, C.; Guo, S. S.; Li, J.; Yang, H. H.; Chen, G. Turn-On Fluorescence Sensor for Intracellular Imaging of Glutathione Using g-C_3N_4 Nanosheet-MnO_2 Sandwich Nanocomposite. *Anal. Chem.* **2014**, *86*, 3426-3434.

(10) Zhang, N.; Qu, F.; Luo, H. Q.; Li, N. B. Sensitive and selective detection of biothiols based on target-induced agglomeration of silver nanoclusters. *Biosens. Bioelectron.* **2013**, *42*, 214-218.

(11) Yang, P.; Xu, Q. Z.; Jin, S. Y.; Zhao, Y.; Lu, Y.; Xu, X. W.; Yu, S. H. Synthesis of Fe_3O_4@Phenol Formaldehyde Resin Core–Shell Nanospheres Loaded with Au Nanoparticles as Magnetic FRET Nanoprobes for Detection of Thiols in Living Cells. *Chemistry* **2012**, *18*, 1154-1160.